Science Signaling
AAAS

www.sciencesignaling.org/cgi/content/full/10/469/eaah3737/DC1

Supplementary Materials for

Cytoskeletal adaptivity regulates T cell receptor signaling

Timothy J. Thauland, Kenneth H. Hu, Marc A. Bruce, Manish J. Butte*

*Corresponding author. Email: mbutte@mednet.ucla.edu

Published 7 March 2017, *Sci. Signal.* **10**, eaah3737 (2017)
DOI: 10.1126/scisignal.aah3737

This PDF file includes:

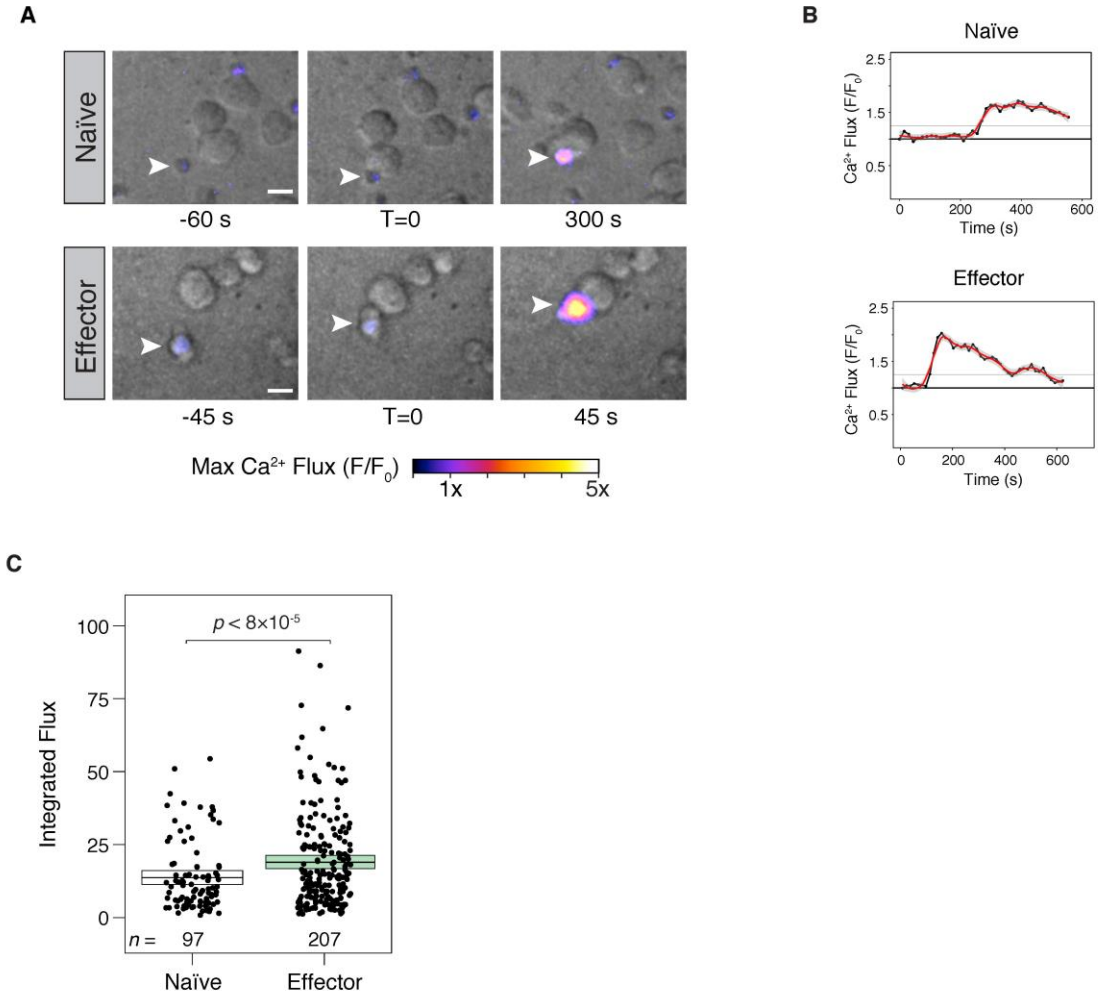

Fig. S1. Ca^{2+} flux measurements in naïve and effector T cells. (**A**) Video microscopy of $CD4^+$ OT-II T cells (arrowheads) loaded with Fluo-4 and dropped near LB27.4 B cells loaded with 1 μM Ova peptide. Ca^{2+} flux is false-colored and scaled according to the brightness of the naïve cell at time zero. Scale bar, 10 μm. (**B**) Representative Ca^{2+} flux curves from a naïve (top) and an effector (bottom) T cell. Time zero represents the time when the T cell entered the field of view. Fluorescence is normalized to that at time zero. These curves were chosen to be closest to the mean degree of Ca^{2+} flux for each population. (**C**) Integrated Ca^{2+} flux ("area under the curve") for naïve and effector T cells. Boxes show means and 95% CI values. Results are representative of two independent experiments.

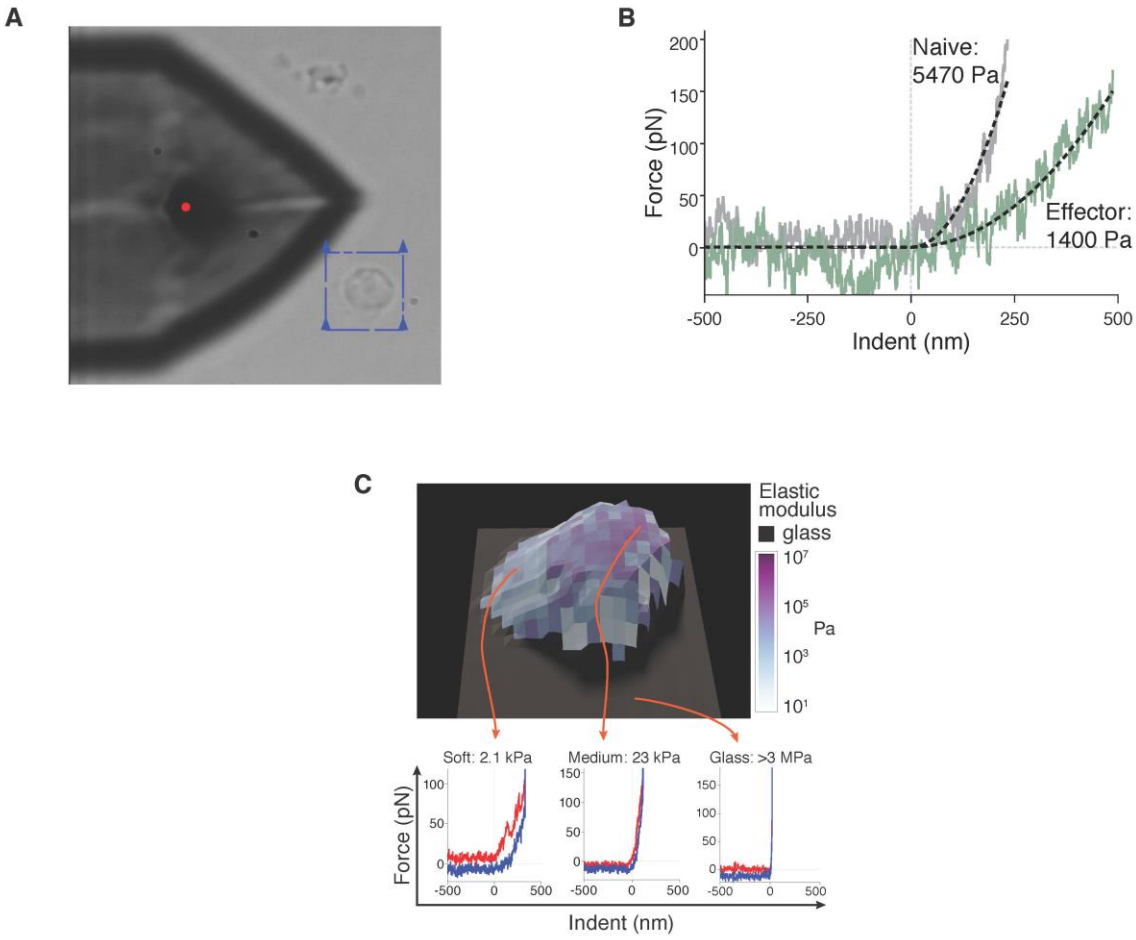

Fig. S2. AFM measurements of T cell stiffness. (**A**) Micrograph showing an AFM cantilever (triangular shape) with its tip (red circle) positioned near a naïve $CD4^+$ T cell (boxed in blue) before making contact. (**B**) Force on the cantilever during the approach and indentation of the tip for representative naïve and effector T cells. Hertz fits are shown in dashed lines. (**C**) Force curves from various points of a naïve $CD4^+$ mouse T cell cultured for 1 hour on a poly-D-lysine–coated glass slide and fixed. Corresponding indentation curves (red, approach curve; blue, retraction curve) are shown for three points together with the elastic moduli obtained by Hertz fitting. Data are representative of xxx experiments.

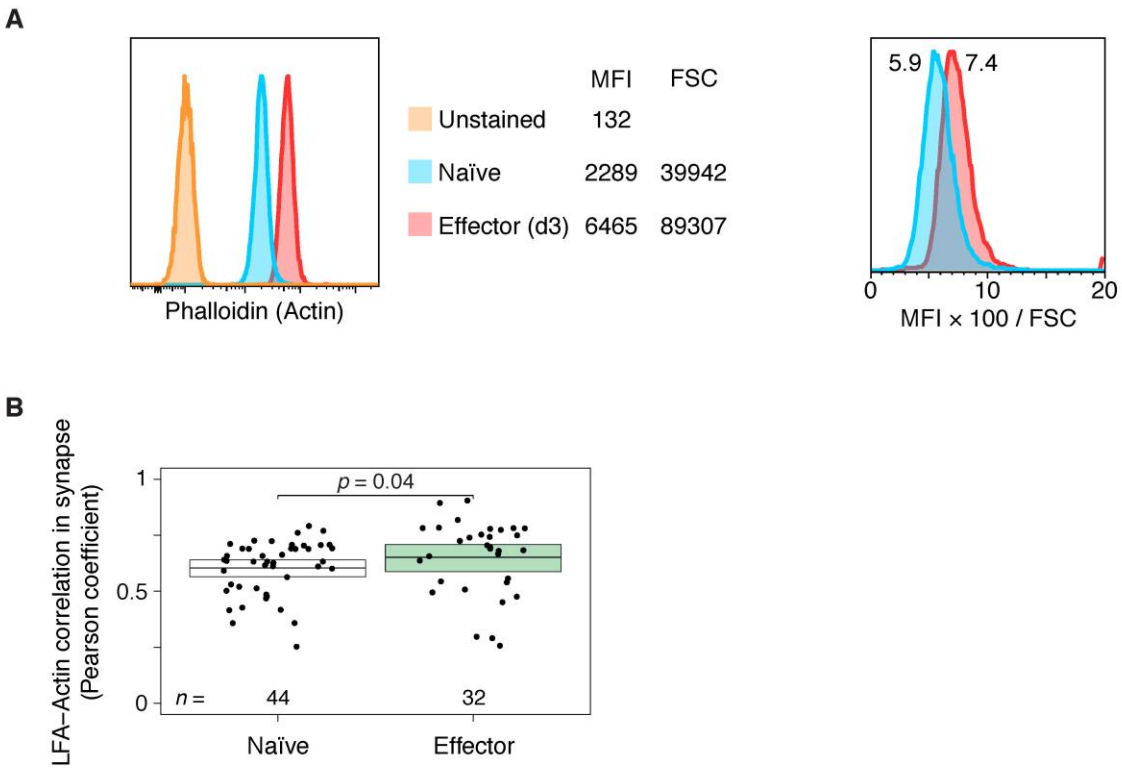

Fig. S3. Naïve and effector T cells have similar amounts of F-actin. (**A**) Naïve and effector $CD4^+$ T cells were fixed, permeabilized, and stained with phalloidin. Effector cells had 1.3-fold more F-actin after normalizing to cell size by forward scatter. Results are representative of two independent experiments. (**B**) Presence of actin in the synapses of naïve and effector T cells was measured by correlation with LFA-1 in the region of LFA-1 enrichment at the synapse. Data are representative of xxx experiments.

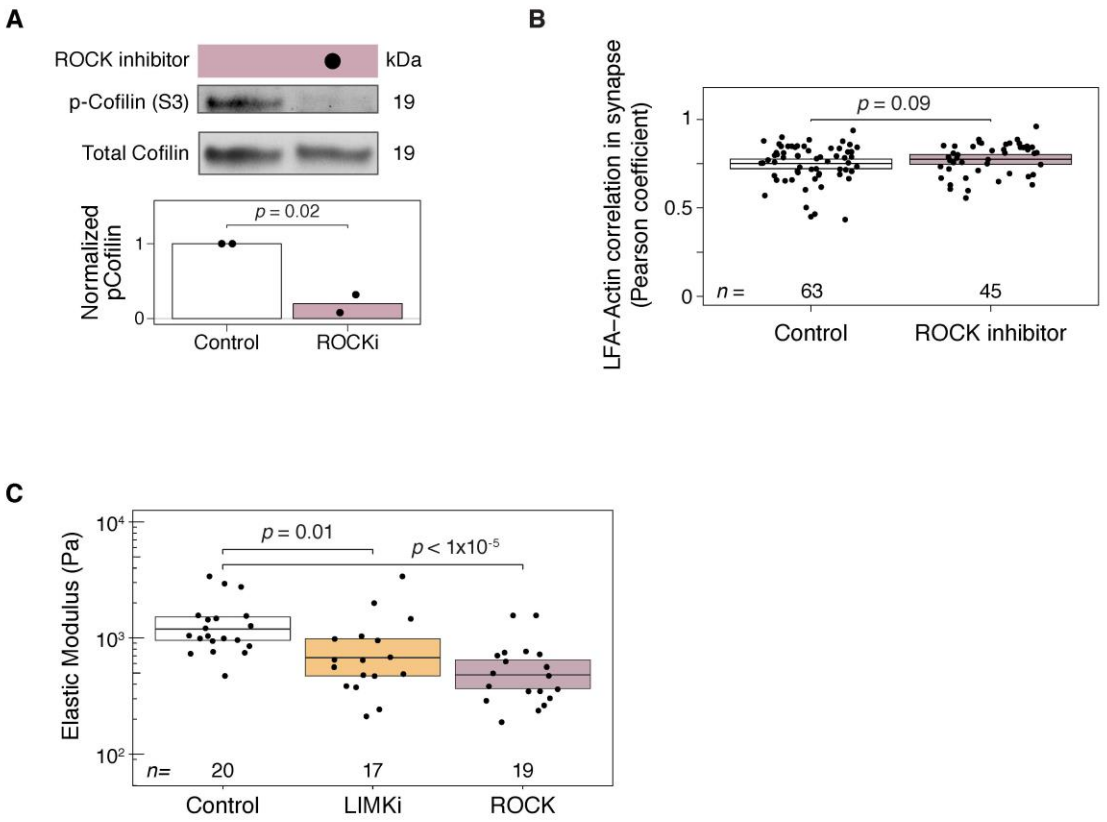

Fig. S4. Inhibiting ROCK reduces cofilin phosphorylation and softens naïve T cells. (**A**) Phosphorylated cofilin (Ser^3, pCofilin) was detected by Western blotting analysis of naïve T cells that were treated for 1 hour with 100 nM glycyl-H-1152 (ROCK inhibitor) or vehicle (DMSO). The amounts of phospho-cofilin were normalized to those of total cofilin. Results are representative of two independent experiments. Bar graph shows densitometric analysis of the relative band intensities. (**B**) The presence of actin in the synapses of naive T cells treated with the ROCK inhibitor or vehicle was measured by correlation with LFA-1 in the region of LFA-1 enrichment at the synapse. (**C**) Naïve B6 $CD4^+$ T cells were treated with the LIMK inhibitor, the ROCK inhibitor, or vehicle for 1 hour and elastic moduli were derived from nanoindentation measurements as described in Fig. 1D. Each dot is the average of ~5 measurements of single T cells. Boxes show means and 95% CI values. Data in (B) and (C) are representative of xxx experiments.

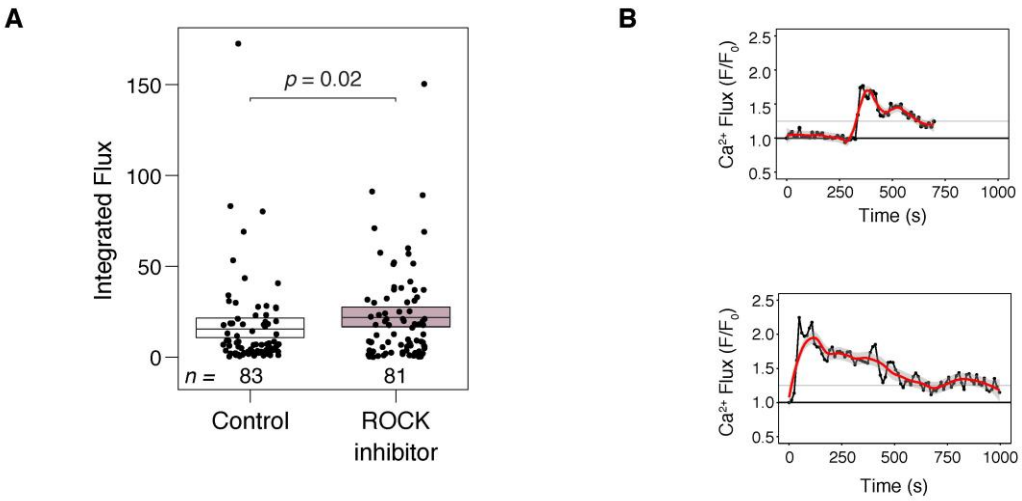

Fig. S5. Inhibiting ROCK enhances Ca^{2+} flux in naïve T cells. (**A**) Integrated Ca^{2+} flux ("area under the curve") measurements for control and ROCK inhibitor treated cells. Boxes show means and 95% CI values. Results are representative of three independent experiments. (**B**) Representative Ca^{2+} flux curves from control and ROCK inhibitor–treated cells from the experiments shown in (A).

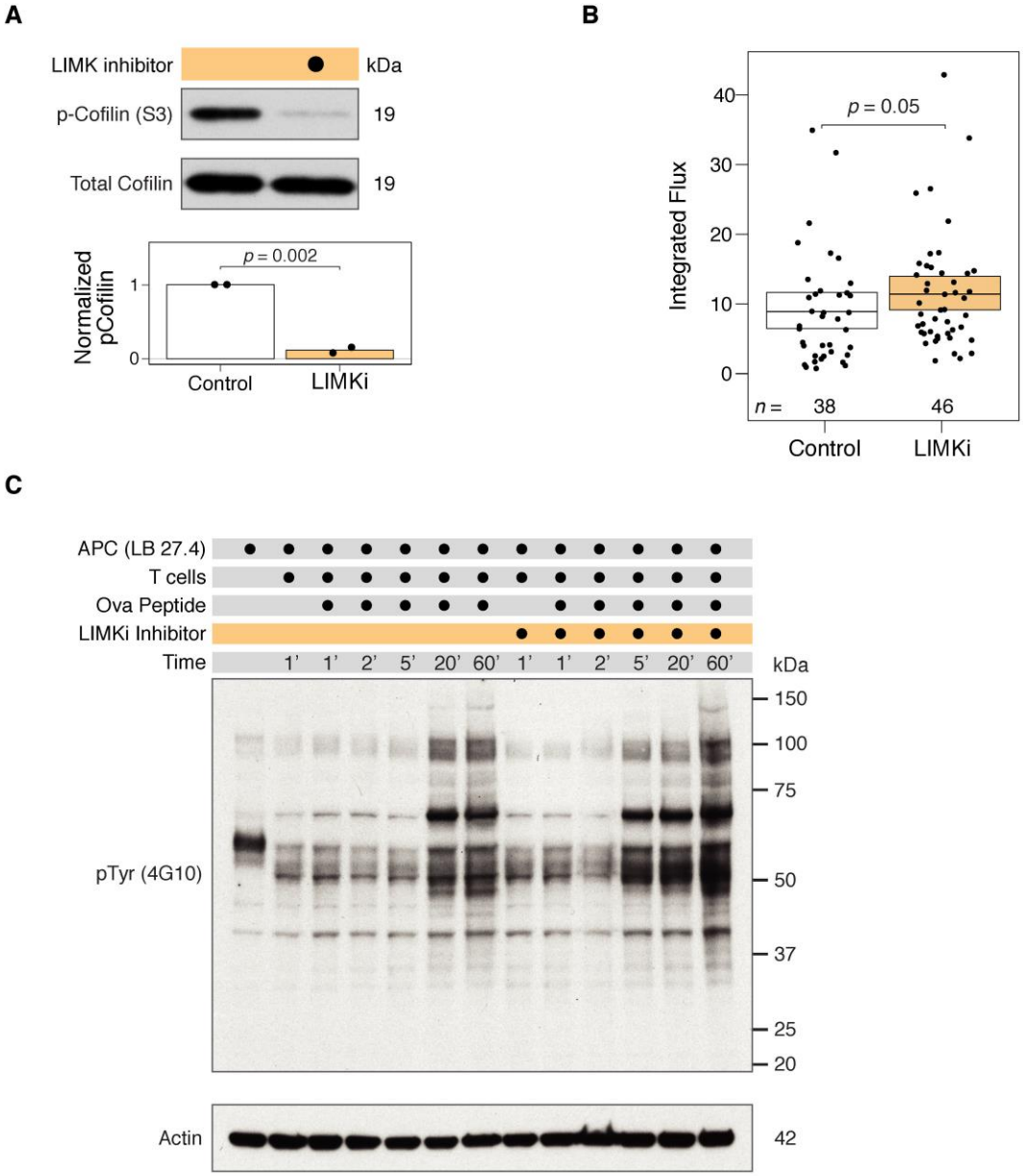

Fig. S6. Inhibiting LIMK reduces cofilin phosphorylation and enhances T cell activation. (**A**) Phospho-cofilin (Ser^3) was detected by Western blotting analysis of naïve T cells that were treated for 1 hour with 1 μM LIMKi 3 (LIMK inhibitor) or vehicle (DMSO). The amounts of phospho-cofilin were normalized to those of total cofilin. Results are representative of two independent experiments. Bar graph shows densitometric analysis of relative band intensities. (**B**) Integrated Ca^{2+} flux ("area under the curve") measurements for control and LIMK inhibitor–treated cells. Boxes show means and 95% CI values. Results are representative of two independent experiments. (**C**) Naïve OT-II T cells were treated with LIMK inhibitor or vehicle for 1 hour and then werer incubated for the indicated times with antigen-pulsed APCs. The samples were then analyzed by Western blotting with an antibody against phosphotyrosine residues. Western blots are representative of xxx experiments.

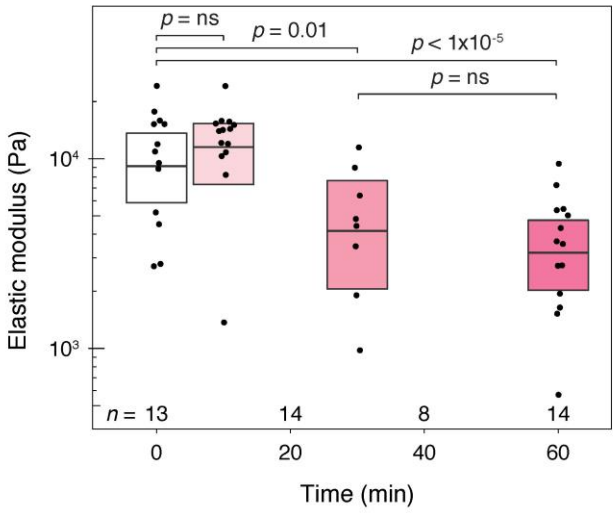

Fig. S7. Time course of the activation-induced softening of T cells. B6 $CD4^+$ T cells were plated on coverslips coated with poly-D-lysine and anti-CD3ε, incubated for 10, 30, or 60 min and then fixed. For time zero, the cells were fixed after a short incubation on poly-D-lysine–coated coverslips. AFM stiffness mapping was performed as described in Fig. 4B. Data are representative of xxx experiments.

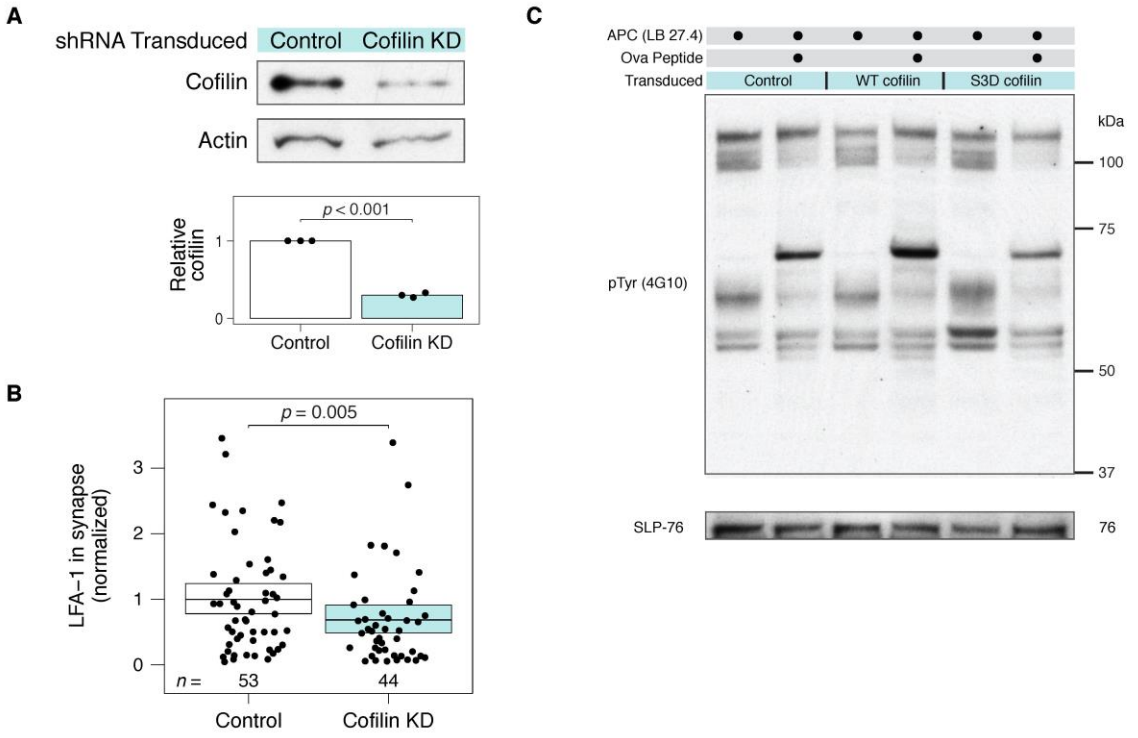

Fig. S8. Cofilin controls immune synapse size and T cell activation. (**A**) OT-II T cells were transduced with control retrovirus or with retrovirus expressing cofilin-specific shRNA and GFP$^+$ cells were sorted on day 3 after activation. Cofilin knockdown was confirmed by Western blotting analysis. Results are representative of three independent experiments. Bar graph shows densitometric analysis of relative band intensities. (**B**) Volume of LFA-1$^+$ voxels in the immune synapse of effector OT-II T cells expressing control or cofilin-specific shRNA and co-cultured for 5 min with antigen-pulsed APCs. Each dot shows an individual T cell–APC immune synapse. Boxes show means and 95% CI values. Results are representative of xxx experiments. (**C**) OT-II T cells were transduced with control retrovirus, retrovirus expressing the S3D cofilin mutant (inactive), or retrovirus expressing WT cofilin (control). The transduced cells were sorted and restimulated with LB27.4 B cells loaded with 1 μM Ova peptide for 5 min. The cells were then analyzed by Western blotting with an antibody specific for phosphotyrosine residues. Results are representative of three independent experiments.

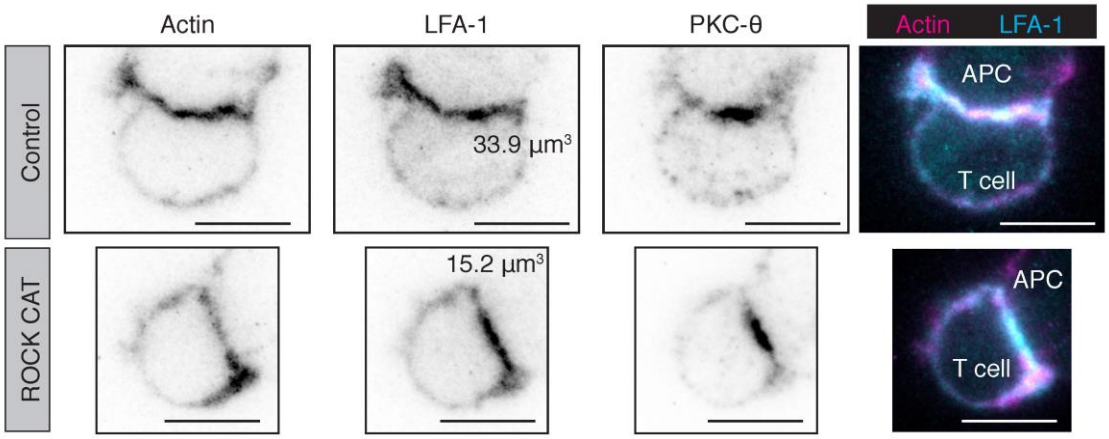

Fig. S9. Examples of immune synapses formed by control T cells and by ROCK CAT–expressing T cells. Immune synapses formed by effector OT-II T cells that were transduced with control retrovirus or with retrovirus expressing the ROCK CAT mutant and then incubated with Ova peptide–pulsed LB27.4 B cells for 5 min as measured by confocal microscopy. Representative cells were chosen near the mean volume of Fig. 5D. Scale bar, 5 µm. Images are representative of xxx experiments.

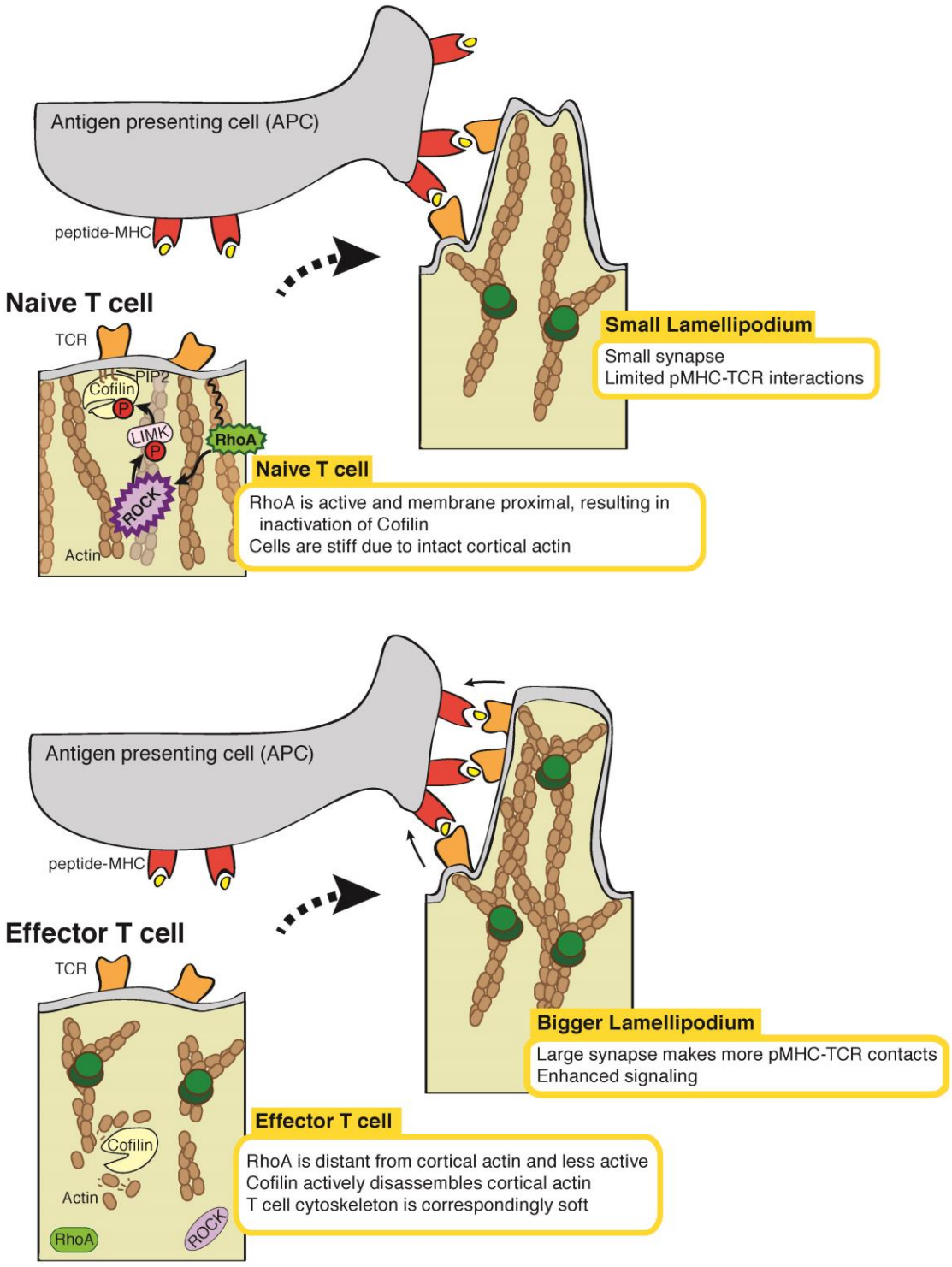

Fig. S10. Model for the control of immune synapse size in T cells by the RhoA-ROCK-LIMK-cofilin axis.

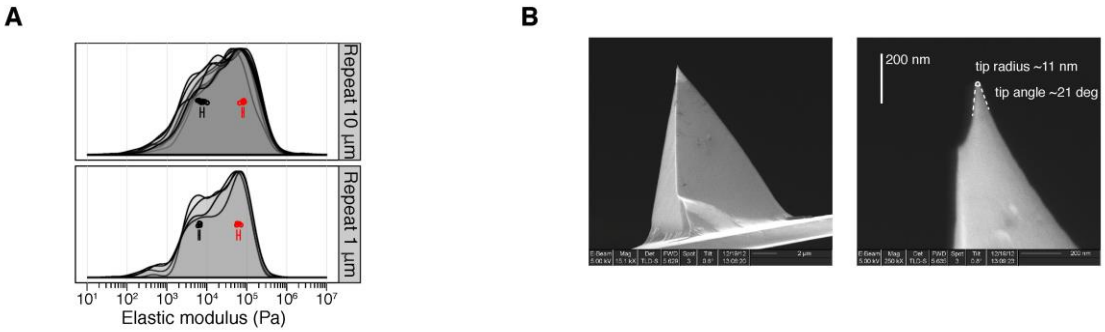

Fig. S11. The cantilever tip is unaffected by repeated scanning. (**A**) To ensure reproducibility of these results, we scanned a single T cell by force mapping repeatedly over ten hours and found no change in measured elastic moduli at either the whole-cell level (P = 0.11 between the first and ninth scans), or when we scanned a 1 μm × 1 μm patch repeatedly (P = 0.31 between the first and fourth scans). Density histograms of elastic moduli from each sequential scan are shown. On another cell, the same 1 μm × 1 μm area was scanned repeatedly and the density histograms of elastic moduli were overlaid. The 25th and 75th percentiles of each distribution are shown in black and red dots, respectively, together with the 95% confidence intervals (bars). (**B**) Scanning electron micrograph images of the cantilever tip after four days of continuous scanning of cells reveals that the tip is as sharp as it was on day zero, based on measurements of tip radius and cone angle.